

Synthetic Approaches to New Redox-Active Carbene Ligands

I. A. Nikovskii^a, K. A. Spiridonov^{a, b}, A. A. Pavlov^a, Yu. V. Nelyubina^{a, c},
K. M. Karnaukh^{a, d}, and A. V. Polezhaev^{a, c, *}

^aNesmeyanov Institute of Organoelement Compounds, Russian Academy of Sciences, Moscow, Russia

^bMoscow State University, Moscow, Russia

^cBauman Moscow State Technical University, Moscow, Russia

^dMoscow Institute of Physics and Technology (National Research University), Dolgoprudnyi, Moscow oblast, Russia

*e-mail: avp@emtc.ru

Received May 2, 2020; revised May 21, 2020; accepted May 25, 2020

Abstract—The design of new redox-switchable molecules requires the development of simple and efficient synthetic approaches. This study demonstrates the possibility of *ortho*-lithiation of ferrocenecarboxaldehyde (aryl)imines (**Ia–Ic**) followed by the reaction with ketones to give 1,2-disubstituted ferrocenes (**IIa–IIc**). These products, in turn, can be cyclized by treatment with trimethylsilyl triflate to give the cationic precursors of ferrocene-containing N-heterocyclic carbenes (**IIIa–IIIc**), in which the heterocycle is annulated to one of the ferrocene cyclopentadienyl ring. Treatment of **IIIa–IIIc** with a base in the presence of a source of rhodium afforded rhodium carbene complexes (**IVa, IVb**) in which the carbene ligand resembled cyclic alkylaminocarbenes in the electron-donor properties. Compounds **Ib** and **IVa** were studied by X-ray diffraction (CIF file CCDC nos. 2000413 and 2000414, respectively).

Keywords: N-heterocyclic carbenes, carbene complexes, transition metal complexes, molecular switches, targeted design, redox-active ligands

DOI: 10.1134/S1070328421020044

INTRODUCTION

The development of advanced smart materials requires introduction, into the molecules, of various functional groups able to change their state in a predicted manner under a particular targeted external action (so-called molecular switches) [1–4]. A simple way of such switching is the reversible change in the oxidation state of one of the atoms in the molecule under the action of electrical potential or an oxidant/reductant [5]. The redox switching can be used in catalysis [6]; nanomedicine [7]; for the design of chemical logic gates [2], sensors [8, 9], transducers [10], or optical elements [8]; in spintronics [11, 12]; and for the design of other smart materials [13]. Redox-switchable catalysis is an atom-economic method in which the catalyst can exist in several catalytically active states with different reactivities, being switched by oxidation/reduction of the ligand. Since these states are derived from the same precursor, the cost of chemical synthesis decreases [6, 14].

In the last two decades, N-heterocyclic carbenes have been gradually replacing the traditional phosphine ligands owing to the unique combination of properties [15, 16], which include facile synthesis, the lack of sensitivity of ligand precursors and complexes to air oxygen and moisture, and strong binding to the metal [17]. This allows for conducting catalysis in air

or at high temperature and pressure if necessary [18, 19]. The drawbacks of these ligands include the relatively narrow range of electron-donor behavior [20] and the generation of moderate (compared with phosphines) steric crowding around the metal atom [21, 22]. Cyclic alkyl(amino) carbenes (CAACs) [23], which have a higher donor ability than the traditional imidazolium and imidazoline carbenes [24] are among the most promising ligands.

Previously, we developed a strategy for the preparation of ferrocene-containing N-heterocyclic carbenes [25] and ferrocene-containing pincer complexes [26–28]. In this work, we utilized this synthetic approach to prepare N-heterocyclic carbenes and their complexes containing an annulated ferrocenyl moiety for their subsequent use in redox-switchable catalysis.

EXPERIMENTAL

All operations involved in the syntheses of complexes were performed in argon in Schlenk vessels using an argon/vacuum line or in dry nitrogen in an MBraun glove box. Commercial organic solvents and chemicals were used. 2,6-Diisopropylaniline, ferrocenecarboxaldehyde, benzophenone, butyllithium, and pyridine (Sigma-Aldrich) were used as received. The solvents were purified by distillation from sodium

with benzophenone or calcium hydride. *N*-(2,6-Dimethylphenyl)-1-ferrocenylmethyleneimine (**Ia**) and *N*-(2,6-diisopropylphenyl)-1-ferrocenylmethyleneimine (**Ic**) were synthesized by a previously described procedure [25]. ^1H , ^{13}C , and ^{19}F NMR spectra were recorded on Bruker Avance 400 and 600 spectrometers (operating at 400 and 600.22 MHz, respectively, for protons). Elemental analysis for carbon, nitrogen, and hydrogen was carried out on a Carlo Erba microanalyzer, design 1106.

Synthesis of *N*-(2,6-diethylphenyl)-1-ferrocenylmethyleneimine (Ib). Ferrocenecarboxaldehyde (2 g, 10.75 mmol) and 2,6-diethylaniline (1.77 mL, 10.75 mmol) were dissolved in toluene (70 mL), and 4 Å molecular sieves (0.5 g) were added. The mixture was refluxed for 8 h. Then the solution was cooled to room temperature and filtered, and toluene was evaporated on a rotary evaporator. The dark red oil was recrystallized twice from petroleum ether to give red crystals. The yield was 2.63 g (71%).

^1H NMR (CD_3CN ; 400 MHz; δ , ppm): 8.27 (s, 1H, CH=N), 7.28 (d, 2H, $J_{\text{HH}} = 7.6$ Hz, ArH), 7.21 (t, 1H, $J_{\text{HH}} = 7.6$ Hz, ArH), 4.98 (s, 2H, C_5H_4), 4.68 (s, 2H, C_5H_4), 4.48 (s, 5H, C_5H_5), 4.27 (q, 4H, $J_{\text{HH}} = 7.5$ Hz, $\text{CH}(\text{CH}_3)_2$), 1.39 (t, 6H, $J_{\text{HH}} = 6.8$ Hz, $\text{CH}(\text{CH}_3)_2$). ^{13}C NMR (CD_3CN ; 100 MHz; δ , ppm): 162.42; 150.73; 133.18; 126.09; 123.59; 70.85; 69.06; 68.69; 24.62; 14.80.

For $\text{C}_{21}\text{H}_{23}\text{NFe}$

Anal. calcd., %	C, 73.05	H, 6.71	N, 4.06
Found, %	C, 73.12	H, 6.81	N, 4.13

General procedure of the synthesis of ferrocenyldiphenylmethanols. The specified ferrocene imine (1.34 mmol) was placed into a 50-mL Schlenk flask and dissolved in 20 mL of THF. The solution was cooled to -78°C , and BuLi (1.1 equiv., 589 μL of a 2.5 M solution in *n*-hexane) was added dropwise. The mixture was slowly warmed up to -20°C . During warming up, a red precipitate of the lithiated product was formed. Then the mixture was cooled to -78°C , and a solution of benzophenone (1.5 mmol) in 5 mL of THF was added dropwise. The cooling bath was removed, and the mixture was warmed up to room temperature and stirred for 1 h. Then several drops of distilled water were added to hydrolyze the lithium salt, and the solvent was removed on a rotary evaporator. The resulting red resinous precipitate was dissolved in dichloromethane, the solution was filtered and concentrated, and the product was recrystallized from *n*-hexane at -10°C .

(2-((2,6-Dimethylphenylimino)methyl)ferrocenyl)diphenylmethanol (IIa) [25]. Yield 0.511 g (65%). ^1H NMR (CD_3CN ; 400 MHz; δ , ppm): 8.40 (s, 1H, OH), 7.96 (s, 1H, CH=N), 7.48 (d, 2H, $J_{\text{HH}} = 7.7$ Hz, ArH), 7.26 (t, 2H, $J_{\text{HH}} = 7.3$ Hz, ArH), 7.17 (t, 1H,

$J_{\text{HH}} = 7.7$ Hz, ArH), 7.03 (s, 5H, ArH), 6.84 (d, 2H, $J_{\text{HH}} = 7.3$ Hz, ArH), 6.75 (t, 1H, $J_{\text{HH}} = 7.3$ Hz, ArH), 4.69 (s, 1H, C_5H_3), 4.42 (s, 1H, C_5H_3), 4.26 (s, 5H, C_5H_5), 3.81 (s, 1H, C_5H_3), 1.65 (s, 6H, CH_3). ^{13}C NMR (CD_3CN ; 100 MHz; δ , ppm): 167.64, 127.86, 127.82, 127.45, 127.19, 126.91, 126.5, 126.34, 123.87, 75.79, 74.64, 70.14, 69.10, 17.35.

For $\text{C}_{34}\text{H}_{33}\text{NOFe}$

Anal. calcd., %	C, 77.02	H, 5.98	N, 2.79
Found, %	C, 76.96	H, 5.85	N, 2.80

(2-((2,6-Diethylphenylimino)methyl)ferrocenyl)diphenylmethanol (IIb). Yield 0.430 g (61%). ^1H NMR (CDCl_3 ; 400 MHz; δ , ppm): 8.50 (s, 1H, OH), 7.94 (s, 1H, CH=N), 7.56 (d, 2H, $J_{\text{HH}} = 7.5$ Hz, ArH), 7.35 (t, 2H, $J_{\text{HH}} = 7.6$ Hz, ArH), 7.27 (t, 1H, $J_{\text{HH}} = 7.5$ Hz, ArH), 7.14 (s, 5H, ArH), 6.98 (s, 3H, ArH), 4.56 (s, 1H, C_5H_3), 4.42 (s, 1H, C_5H_3), 4.36 (s, 5H, C_5H_5), 3.95 (s, 1H, C_5H_3), 2.04 (q, 4H, $J_{\text{HH}} = 7.6$ Hz, 2CH_2), 0.86 (t, 6H, $J_{\text{HH}} = 7.6$ Hz, CH_3). ^{13}C NMR (CDCl_3 ; 100 MHz; δ , ppm): 166.46, 127.89, 127.56, 127.38, 127.10, 126.59, 126.52, 125.82, 124.31, 77.12, 76.05, 74.75, 74.28, 70.17, 69.00, 24.10, 14.82.

For $\text{C}_{34}\text{H}_{33}\text{NOFe}$

Anal. calcd., %	C, 77.42	H, 6.31	N, 2.66
Found, %	C, 77.53	H, 6.35	N, 2.68

(2-((2,6-Diisopropylphenylimino)methyl)ferrocenyl)diphenylmethanol (IIc) [25]. Yield 0.740 g (72%). ^1H NMR (CD_3CN ; 400 MHz; δ , ppm): 8.28 (s, 1H, OH), 7.95 (s, 1H, CH=N), 7.45 (d, 2H, $J_{\text{HH}} = 7.75$ Hz, ArH), 7.26 (t, 2H, $J_{\text{HH}} = 7.37$ Hz, ArH), 7.26 (t, 1H, $J_{\text{HH}} = 7.75$ Hz, ArH), 7.07 (m, 3H, ArH), 7.00 (t, 2H, $J_{\text{HH}} = 3.53$ Hz, ArH), 6.93 (m, 3H, ArH), 4.74 (s, 1H, C_5H_3), 4.46 (s, 1H, C_5H_3), 4.25 (s, 5H, C_5H_5), 3.86 (s, 1H, C_5H_3), 2.82 (m, 2H, $\text{CH}(\text{CH}_3)_2$), 0.86 (d, 12H, $\text{CH}(\text{CH}_3)_2$). ^{13}C NMR (CD_3CN ; 100 MHz; δ , ppm): 167.32, 127.88, 127.34, 127.27, 126.86, 126.56, 126.48, 124.54, 122.65, 75.72, 74.95, 69.97, 69.29, 27.07, 23.64, 22.62.

Synthesis of (2-((2,6-diisopropylphenylimino)methyl)ferrocenyl)diphenylethanol (IIId). *N*-(2,6-Diisopropylphenyl)-1-ferrocenylmethyleneimine (0.372 g, 0.67 mmol) and 20 mL of THF were placed into a 50-mL Schlenk flask. The solution was cooled to -78°C , and BuLi (1.1 equiv., 294 μL of a 2.5 M solution in *n*-hexane) was added dropwise. The mixture was slowly warmed up to -20°C . During warming up, a red precipitate of the lithiation product was formed. Then the mixture was cooled to -78°C , and a solution of 1,1-diphenyloxirane (0.147 g, 0.75 mmol) in 5 mL of THF was added dropwise. The cooling bath was removed, and the mixture was warmed up to room

temperature and stirred for 1 h. Then several drops of distilled water were added to hydrolyze the lithium salt, and the solvent was removed on a rotary evaporator. The resulting red resinous precipitate was dissolved in dichloromethane, and the solution was filtered and concentrated. The product was purified by column chromatography (elution with toluene–hexane (1 : 1)). The yield was 0.017 g (13%). ¹H NMR (CD₃CN; 400 MHz; δ, ppm): 8.25 (s, 1H, CH=N), 7.83 (d, 1H, ArH), 7.64 (d, 2H, ArH), 7.56 (t, 1H, ArH), 7.51 (d, 2H, ArH), 7.29–7.32 (m, 5H, ArH), 7.23 (d, 2H, ArH), 4.62 (s, 1H, C₅H₃), 4.29 (s, 5H, C₅H₃), 4.25 (s, 1H, C₅H₃), 3.98 (s, 1H, C₅H₃), 3.96 (s, 2H, CH₂), 3.12 (sept., 2H, *J*_{HH} = 6.9 Hz, CH), 1.28 (d, 12H, *J*_{HH} = 6.9 Hz, CH(CH₃)₂), 1.14 (d, 12H, *J*_{HH} = 6.9 Hz, CH(CH₃)₂).

For C₃₇H₃₉NOFe

Anal. calcd., %	C, 78.02	H, 6.90	N, 2.46
Found, %	C, 78.10	H, 6.81	N, 2.38

General procedure for the synthesis of imidazolium carbene precursors. In a glove box, specified diphenylmethanol (1.8 mmol) was dissolved in 5 mL of CH₂Cl₂ in a 20-mL vial, and pyridine (0.5 mL) was added. The resulting solution was cooled to –78°C, and trifluoromethanesulfonic anhydride (82 μL, 0.486 mmol) was added dropwise. The reaction mixture was stirred for 40 min at room temperature. During stirring, the color of the reaction mixture slowly changed from dark red to bright violet. Then 15 mL of *n*-hexane was added to the resulting solution, and a precipitate formed. The solution was decanted, and the precipitate was washed with *n*-hexane and dissolved in 5 mL of CH₂Cl₂. The solution was cooled to –78°C and filtered to remove the precipitated pyridinium salt, 15 mL of *n*-hexane was added, and the solution was decanted. The bright violet precipitate was dried in a high vacuum.

6-(2,6-Dimethylphenyl)-5,5-diphenyl-5H-pyrrolo[3,4-a]ferrocen-6-ium trifluoromethanesulfonate (IIIa). Yield: 0.734 g (45%). ¹H NMR (acetone-d₆; 600 MHz; δ, ppm): 10.10 (s, 1H, CH = N), 7.77 (d, 2H *J*_{HH} = 7.4 Hz, *o*-Ph'), 7.64 (t, 1H, *J*_{HH} = 7.4 Hz, *p*-Ph'), 7.55 (t, 2H, *J*_{HH} = 7.4 Hz, *m*-Ph'), 7.44 (t, 1H, *J*_{HH} = 7.6 Hz, *p*-PhMe₂), 7.39 (t, 1H, *J*_{HH} = 7.8 Hz, *p*-Ph), 7.29 (t, 2H, *J*_{HH} = 7.8 Hz, *m*-Ph), 7.20–7.17 (m, 2H, *m*-PhMe₂), 6.90 (d, 2H, *J*_{HH} = 7.8 Hz, *o*-Ph), 5.65 (s, 2H, C₅H₃), 5.42 (s, 1H, C₅H₃), 4.7 (s, 5H, C₅H₃), 1.85 (s, 1H, Me), 1.45 (s, 1H, Me). ¹³C NMR (acetone-d₆; 150.9 MHz; δ, ppm): 181.27, 137.80, 137.46, 135.41, 131.90, 131.07, 130.20, 130.09, 129.89, 128.96, 128.82, 127.92, 127.64, 127.33, 102.90, 88.91, 81.94, 80.80, 73.26, 71.33, 66.38, 18.50, 18.38. ¹⁹F

NMR (acetone-d₆, 376 MHz; δ, ppm): = –78.67 (s, 3F, TfO).

For C₃₃H₂₈NF₃O₃SFe

Anal. calcd., %	C, 62.77	H, 4.47	N, 2.22
Found, %	C, 62.85	H, 4.56	N, 2.35

6-(2,6-Diethylphenyl)-5,5-diphenyl-5H-pyrrolo[3,4-a]ferrocen-6-ium trifluoromethanesulfonate (IIIb). Yield 0.569 g (48%). ¹H NMR (CD₂Cl₂; 400 MHz; δ, ppm): 9.76 (s, 1H, CH=N), 7.60–7.51 (m, 3H, Ph), 7.48 (t, 1H, *J*_{HH} = 7.7 Hz, Ph(Et)₂), 7.16 (t, 2H, *J*_{HH} = 7.8 Hz, Ph), 7.33–7.28 (m, 2H, Ph(Et)₂), 7.20–7.14 (m, 4H, Ph), 6.71 (d, 1H, *J*_{HH} = 7.7 Hz, Ph), 5.63 (s, 1H, C₅H₃), 5.43 (s, 1H, C₅H₃), 5.04 (s, 1H, C₅H₃), 4.58 (s, 5H, C₅H₃), 2.15 (sext., 1H, *J*_{HH} = 7.4 Hz, Et), 1.87 (sext., 1H, *J*_{HH} = 7.7 Hz, Et), 1.67 (sext., 1H, *J*_{HH} = 7.7 Hz, Et), 1.54 (sext., 1H, *J*_{HH} = 7.4 Hz, Et), 0.92 (t, 3H, *J*_{HH} = 7.7 Hz, Et), 0.63 (t, 3H, *J*_{HH} = 7.4 Hz, Et). ¹³C NMR (CD₂Cl₂; 100 MHz; δ, ppm): 180.53, 143.03, 140.64, 137.01, 135.55, 131.40, 130.05, 129.92, 128.75, 128.64, 127.96, 127.75, 126.62, 102.43, 89.55, 81.78, 80.79, 73.20, 70.85, 66.87, 24.37; 13.97, 13.59. ¹⁹F NMR (CD₂Cl₂; 376 MHz; δ, ppm): –78.62 (s, 3F, TfO).

For C₃₅H₃₂NF₃O₃SFe

Anal. calcd., %	C, 63.74	H, 4.89	N, 2.12
Found, %	C, 63.81	H, 4.96	N, 2.03

6-(2,6-Diisopropylphenyl)-5,5-diphenyl-5H-pyrrolo[3,4-a]ferrocen-6-ium trifluoromethanesulfonate (IIIc). Yield 0.668 g (54%). ¹H NMR (CD₂Cl₂; 600 MHz; δ, ppm): 9.89 (s, 1H, CH=N), 7.53–7.44 (m, 6H, Ph), 7.25 (t, 2H, *J*_{HH} = 7.9 Hz, Ph(iPr)₂), 7.16 (t, 3H, *J*_{HH} = 8.4 Hz, Ph), 6.65 (d, 2H, *J*_{HH} = 7.9 Hz, Ph(iPr)₂), 5.69 (s, 1H, C₅H₃), 5.40 (s, 1H, C₅H₃), 4.90 (s, 1H, C₅H₃), 4.62 (s, 5H, C₅H₃), 2.44 (pent., 1H, *J*_{HH} = 5.9 Hz, CH(CH₃)₂), 2.24 (pent., 1H, *J*_{HH} = 6.6 Hz, CH(CH₃)₂), 1.05 (dd, 6H, *J*_{HH} = 5.9 Hz, *J*_{HH} = 83 Hz, CH(CH₃)₂), 0.32 (dd, 6H, *J*_{HH} = 6.6 Hz, *J*_{HH} = 25.5 Hz, CH(CH₃)₂). ¹³C NMR (CD₂Cl₂; 150.9 MHz; δ, ppm): 181.04; 148.78, 146.17, 137.77, 133.33, 132.40, 131.27, 130.81, 130.32, 129.18, 128.65, 126.34, 125.28, 102.41, 90.07, 81.97, 81.19, 69.97, 67.26, 53.47, 29.91, 29.25, 26.80, 25.24, 21.46, 20.54. ¹⁹F NMR (CD₂Cl₂; 376 MHz; δ, ppm): –78.64 (s, 3F, TfO).

For C₃₇H₃₆NF₃O₃SFe

Anal. calcd., %	C, 64.63	H, 5.28	N, 2.04
Found, %	C, 64.69	H, 5.37	N, 2.08

General procedure for the synthesis of rhodium carbene complexes. In a glove box, lithium bis(trimethylsilyl)amide (85 mg, 0.51 mmol), rhodium cycloocta-

diene chloride dimer (200 mg, 0.51 mmol), and the specified imidazolium carbene precursor (0.25 mmol) were mixed in a 20 mL vial. The dry mixture was cooled to -78°C , and THF was added. The resulting solution was stirred at -78°C for 30 min, warmed up to room temperature, and stirred for additional 30 min. The obtained complex was purified by column chromatography (elution with petroleum ether–ethyl acetate (5 : 1)).

Chlorocyclooctadiene [2-(2,6-dimethylphenyl)-3,3-diphenylferrocenylpyrrol-2-ylidene]rhodium (IVa). Yield 41 mg (23%). ^1H NMR (CDCl_3 ; 600 MHz; δ , ppm): 7.65 (s, 2H, *o*-Ph), 7.43 (t, 1H, *p*-Ph/*p*-PhMe₂), 7.30 (t, 2H, $J_{\text{HH}} = 7.4$ Hz, *m*-Ph), 7.23 (t, 1H, $J_{\text{HH}} = 7.4$ Hz, *p*-Ph/*p*-PhMe₂), 7.05–7.12 (m, 4H, *m*-Ph + *m*-PhMe₂), 6.97 (d, 2H, $J_{\text{HH}} = 7.6$ Hz, *o*-Ph), 6.83 (d, 1H, $J_{\text{HH}} = 7.4$ Hz, *p*-Ph), 5.51 (s, 1H, C₅H₃), 5.13 (m, 1H, C₈H₁₂), 4.89 (m, 1H, C₈H₁₂), 5.79 (s, 1H, C₅H₃), 4.36 (s, 5H, C₅H₅), 4.26 (m, 1H, C₈H₁₂), 4.18 (s, 1H, C₅H₃), 2.96 (m, 1H, C₈H₁₂), 2.64 (m, 1H, C₈H₁₂), 2.28 (m, 1H, C₈H₁₂), 2.12 (m, 1H, C₈H₁₂), 1.93 (m, 1H, C₈H₁₂), 1.86–1.78 (m, 2H, C₈H₁₂), 1.53 (m, 2H, C₈H₁₂). ^{13}C NMR (CDCl_3 ; 150.9 MHz; δ , ppm): 252.74 (d., $J_{\text{CRh}} = 43.3$ Hz), 141.75, 141.33, 139.04, 138.16, 134.05, 131.32, 129.98, 129.41, 129.70, 128.66, 127.91, 127.73, 127.42, 126.84, 100.37 (d, $J_{\text{CRh}} = 5.7$ Hz), 99.88 (d, $J_{\text{CRh}} = 5.7$ Hz), 98.64, 96.17, 88.36, 75.94, 70.59, 69.67 ($J_{\text{CRh}} = 14.4$ Hz), 67.85 ($J_{\text{CRh}} = 14.4$ Hz); 66.80, 62.67, 34.61, 31.70, 31.55, 29.40, 27.59, 22.77, 21.33, 18.96.

For C₄₂H₄₆NCIFeRh

Anal. calcd., %	C, 66.46	H, 6.11	N, 1.85
Found, %	C, 66.11	H, 6.89	N, 1.99

Chlorocyclooctadiene [2-(2,6-diethylphenyl)-3,3-diphenylferrocenylpyrrol-2-ylidene]rhodium (IVb). Yield 35 mg (19%). ^1H NMR (CDCl_3 ; 600 MHz; δ , ppm): 7.36–7.46 (m, 2H, Ph), 7.37 (t, 2H, $J_{\text{HH}} = 7.1$ Hz, Ph), 7.29–7.33 (m, 2H, Ph), 7.07 (d, 2H, $J_{\text{HH}} = 6.5$ Hz, Ph), 7.04 (t, 2H, $J_{\text{HH}} = 7.7$ Hz, Ph), 6.95–6.98 (m, 3H, Ph), 5.50 (s, 1H, C₅H₃), 5.14 (m, 1H, C₈H₁₂), 4.92 (m, 1H, C₈H₁₂), 4.78 (s, 1H, C₅H₃), 4.38 (s, 5H, C₅H₅), 4.18 (m, 1H, C₈H₁₂), 3.68 (s, 5H, C₅H₅), 2.85 (sext., 1H, $J_{\text{HH}} = 7.8$ Hz, Et), 2.64 (m, 1H, C₈H₁₂), 2.24 (m, 1H, C₈H₁₂), 2.13 (m, 1H, C₈H₁₂), 1.93 (m, 4H, C₈H₁₂ + 2Et), 1.50 (m, 2H, C₈H₁₂), 0.70 (t, 3H, $J_{\text{HH}} = 7.3$ Hz, Et), 0.63 (t, 3H, $J_{\text{HH}} = 7.3$ Hz, Et). ^{13}C NMR (CDCl_3 ; 150.9 MHz; δ , ppm): 252.92 (d, $J_{\text{CRh}} = 43.3$ Hz), 143.86, 143.29, 140.94, 140.27, 134.10, 131.26, 129.26, 128.76, 128.71, 128.65, 127.75, 127.59, 126.87, 123.63, 100.27 (d, $J_{\text{CRh}} = 5.1$ Hz); 99.79 (d, $J_{\text{CRh}} = 5.6$ Hz); 98.33, 96.03, 88.56, 75.86, 70.29, 69.95 ($J_{\text{CRh}} = 13.6$ Hz), 67.86 ($J_{\text{CRh}} = 14.8$ Hz), 66.71, 62.46, 34.67, 31.62, 31.39,

29.45, 28.04, 27.35, 25.36, 24.13, 22.69, 14.95, 14.18, 11.77.

For C₄₂H₄₃NCIFeRh

Anal. calcd., %	C, 66.73	H, 5.73	N, 1.85
Found, %	C, 66.81	H, 5.64	N, 1.92

X-ray diffraction study of single crystals of **Ib** and **IVa** prepared by slow evaporation in air from a solution in hexane (**Ib**) or a 1 : 1 hexane–dichloromethane mixture (**IVa**) was carried out on a Bruker APEX2 CCD diffractometer (MoK α radiation, graphite monochromator, ω -scan mode). The structures were solved using the ShelXT software [29] and refined by least squares in the full-matrix anisotropic approximation on F_{hkl}^2 using the Olex2 software [30]. The positions of hydrogen atoms were calculated geometrically and refined in the isotropic approximation by the riding model. Selected crystallographic data and refinement details are summarized in Table 1.

The structural data for compounds **Ib** and **IVa** are deposited with the Cambridge Crystallographic Data Centre (CCDC nos. 2000413 and 2000414; <http://www.ccdc.cam.ac.uk/>).

RESULTS AND DISCUSSION

A number of carbenes and carbene-based complexes containing a ferrocene moiety were reported in the literature [31, 32]. It is noteworthy that in most compounds of this type, the ferrocenylmethyl substituent is located on the nitrogen atom and is separated from the carbene carbon atom by several non-conjugated bonds [31]. As a result, oxidation or reduction of the ferrocene moiety has virtually no effect on the electron-donor ability of the ligand, which makes this synthetic design inappropriate for redox-switchable systems in which the redox moiety is supposed to directly affect the electron-donor ability of the ligand. Previously, we developed a facile synthetic route to precursors of a carbene ligand [25, 33, 34] with heterocyclic ring being annulated to the metallocene moiety, which was potentially suitable for directly affecting the carbene center.

It was shown [25] that butyllithium is able to efficiently lithiate ferroceneimines in the *ortho*-position to the imino group without any noticeable addition at the electrophilic imine carbon atom. In this study, we extended the range of imines by using diethylaniline derivative in order to attain a better solubility of carbene complexes in organic solvents. For this purpose, we prepared a series of *N*-(2,6-dialkylphenyl)-1-ferrocenylmethyleneimines (**Ia–Ic**) by the procedure proposed previously. The obtained compounds were characterized in detail using a set of physicochemical methods, including X-ray diffraction. In particular, the crystal structure of compound **Ib** was proved

Table 1. Key crystallographic data and structure refinement parameters for **Ib** and **IVa**

Parameter	Value	
	Ib	IVa
<i>M</i>	345.25	771.02
<i>T</i> , K	120	120
System	Orthorhombic	Triclinic
Space group	<i>Pbca</i>	<i>P</i> $\bar{1}$
<i>Z</i>	16	2
<i>a</i> , Å	9.8084(8)	10.060(4)
<i>b</i> , Å	15.2180(12)	10.963(4)
<i>c</i> , Å	45.882(4)	17.157(7)
α , deg	90.00	88.353(9)
β , deg	90.00	81.334(9)
γ , deg	90.00	67.954(8)
<i>V</i> , Å ³	6848.5(10)	1733.1(12)
ρ (calcd.), g cm ⁻³	1.339	1.478
μ , cm ⁻¹	8.80	10.04
<i>F</i> (000)	2912	798
$2\theta_{\max}$, deg	54	54
Number of measured reflections	61778	18483
Number of unique reflections (<i>R</i> _{int})	7485 (0.1102)	7537 (0.1505)
Number of reflections with <i>I</i> > 2 σ (<i>I</i>)	5362	3939
Number of refined parameters	419	427
<i>R</i> ₁ , <i>wR</i> ₂ (<i>I</i> > 2 σ (<i>I</i>))	0.0530, 0.0917	0.0673, 0.1207
<i>R</i> ₁ , <i>wR</i> ₂ (all data)	0.0861, 0.1043	0.1508, 0.1547
GOOF	1.084	0.953
$\Delta\rho_{\max}/\Delta\rho_{\min}$, e Å ⁻³	0.498/−0.655	0.987/−0.885

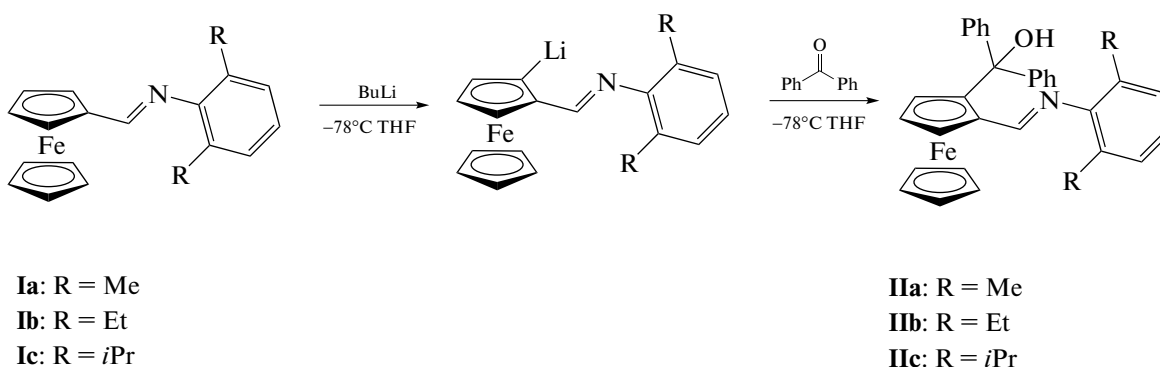
(Fig. 1) to contain two symmetrically independent complex molecules, which almost did not differ in the geometric parameters (Table 2). In both cases, the $-\text{C}(\text{H})=\text{N}-$ group was located nearly in the plane of the cyclopentadienyl ring, as indicated by the fact that the angle between these planes was less than 11° . For comparison, the angles between two ferrocene cyclopentadienyl rings in the two symmetrically independent molecules of the complex were $3.93(14)^\circ$ and $3.68(14)^\circ$. Conversely, 2,6-dimethyl-substituted phenyl group was rotated relative to the $-\text{C}(\text{H})=\text{N}-$ group by $68.82(10)^\circ$ and $78.65(10)^\circ$, respectively, due to the presence of bulky ethyl substituents in the *ortho*-positions of the benzene ring. This is apparently responsible for the fact that stacking interactions, which could be expected to occur between the aromatic groups of various types (cyclopentadienyl ligands, phenyl groups, and even the $-\text{C}(\text{H})=\text{N}-$ groups) present in this complex, were absent in the crystal of **Ib**.

All of the obtained imines were successfully *ortho*-lithiated by a previously described procedure [25], and the products were allowed to react with benzophenone to give 1,2-disubstituted ferrocenes (Scheme 1).

Table 2. Selected geometric parameters of compound **Ib** according to X-ray diffraction data at 120 K*

Parameter	Value
Fe–C(Cp), Å	2.037(3)–2.058(3)
α , deg	3.93(14), 3.68(14)
β , deg	11.00(12), 7.72(12)
γ , deg	68.82(10), 78.65(10)

* C(Cp) stands for carbon atoms of the cyclopentadienyl rings; α is the angle between their root-mean square planes, β and γ are the angles of rotation of the $-\text{C}(\text{H})=\text{N}-$ group relative to the cyclopentadienyl ring and phenyl ring planes, respectively.



Scheme 1.

The yield of compound **IIIb** proved to be lower than the yields of **IIa** and **IIIc**, because of its better solubility, which hampered isolation of **IIIb** in a pure state by crystallization. Ferrocenyldiphenylmethanols **IIa–IIIc** can undergo intramolecular cyclization, with carbocation being generated upon protonation of the hydroxyl group, followed by water elimination. This gives a pyrrolium ring annulated to cyclopentadienyl ring (Scheme 2). Although the new ring contains five atoms, it is highly strained, in particular, due to repulsion between bulky substituents in the aryl moiety and unsubstituted cyclopentadienyl moiety. This affects the stability of carbene precursors and makes them prone to hydrolysis and, possibly, affects the stability of the complexes. In order to eliminate the ring strain,

we proposed an approach to ring expansion by one carbon atom using 1,1-diphenyloxirane as the electrophile in the reaction with lithium salt.

However, we failed to attain a high yield of **IIIId** (at most 13%) or a high reactant conversion, which was mainly related to low reactivity of 1,1-diphenyloxirane towards nucleophiles. Attempts to solve this problem by adding copper salts and various chelating agents also failed.

Cyclization of ferrocenyldiphenylmethanols to pyrrolium salts was induced by trifluoromethanesulfonic acid in the presence of pyridine at -78°C (Scheme 2).

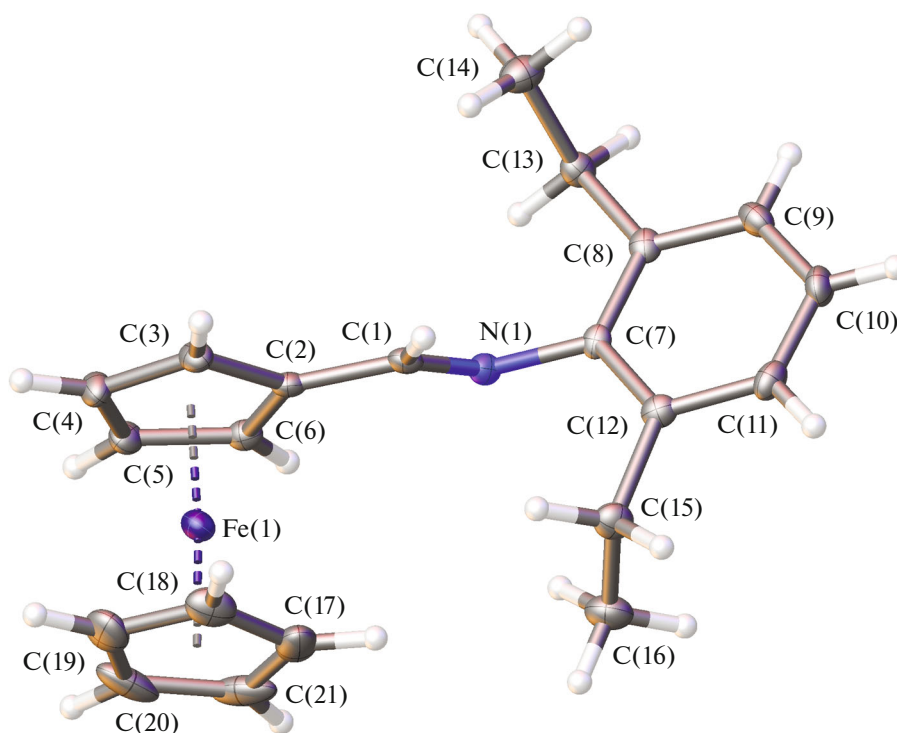
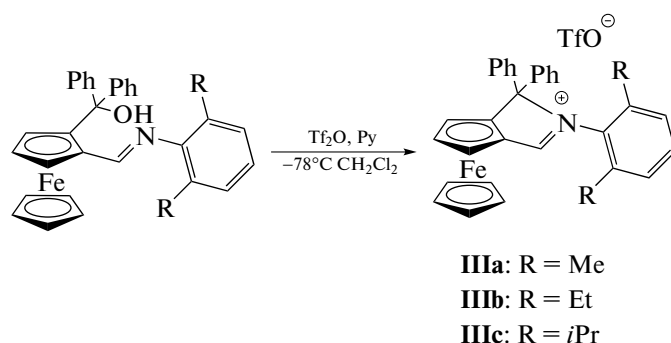


Fig. 1. General view of complex **IIb** with atoms being represented by thermal ellipsoids ($p = 50\%$).

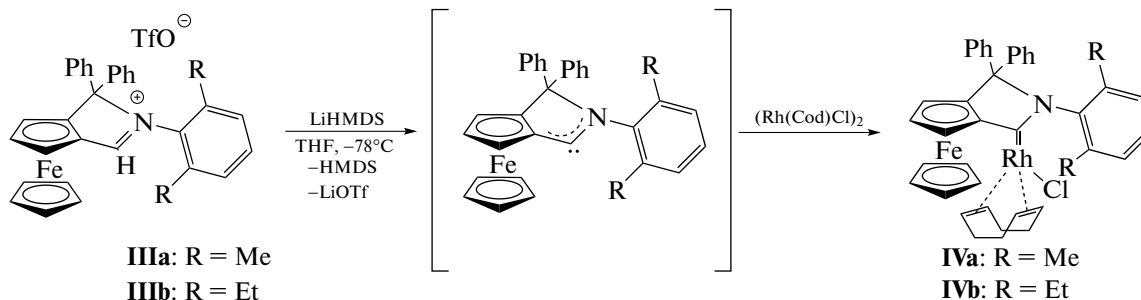


Scheme 2.

The use of sodium hydride, butyllithium, or lithium bis(trimethylsilyl)amide as bases also produces the target product; however, isolation of the product with this synthetic protocol is difficult due to numerous side reactions. The use of pyridine as a base results in the formation of pyridinium trifluoromethanesulfonate by-product, which is poorly soluble in dichloromethane and can be separated by filtration. Products **IIIa–IIIc** are rapidly hydrolyzed by air moisture and are unstable in solutions even under inert conditions. The formation of these compounds as the only reaction products is indicated by the data of NMR spectroscopy. The ^1H NMR spectrum exhibits a signal of the only proton of the pyrrolium ring at 9.76–10.10 ppm, while the ^{13}C NMR spectrum shows a signal for the carbon atom bound to this ring at 180.53–181.27 ppm, which markedly differs from the signals of the precursor imino group (7.94–7.96 and 166.46–167.64 ppm in the ^1H and ^{13}C NMR spectra, respectively). The signal for the hydroxyl group proton

disappeared. The *ortho*-substituents in the aryl moiety become non-equivalent due to impossibility of rotation around the $\text{C}_{\text{Ar}}-\text{N}$ bond, which is manifested as a double set of NMR signals (1.85 and 1.45 ppm for **IIIa**). The ^{19}F NMR spectrum shows a singlet at -79.5 ppm, which confirms the presence of a free triflate anion. Elemental analysis data are consistent with the proposed structure of the reaction products.

We used the synthesized pyrrolium salts to generate carbenes *in situ* and for the subsequent reaction with the rhodium complex $[\text{Rh}(\text{Cod})_2\text{Cl}]_2$ (Scheme 3). As the bases, we used potassium *tert*-butoxide and lithium bis(trimethylsilyl)amide. In both cases, we were able to isolate the final product for precursors containing methyl and ethyl substituents. In the case of compound **IIIc**, we could not isolate the target product, which is most likely attributable to the steric hindrance experienced by this complex.



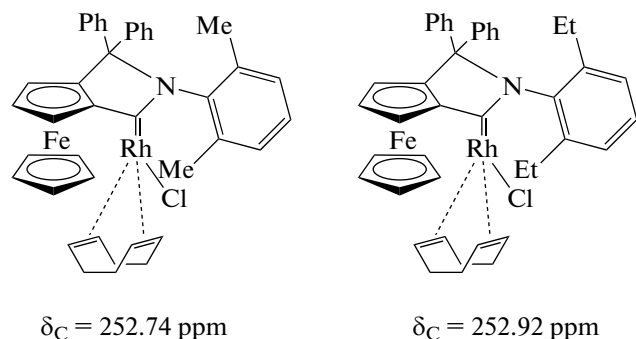
Scheme 3.

We optimized the metallation step by varying the number of moles of the base and thus increased the yield of **IVa** from 7 to 23%. The use of two moles of the base and two moles of the starting diene complex gave the maximum yield. Further increase in the amount of the base did not increase the yield of the target product. Air-stable carbene complexes were characterized by NMR spectroscopy. The proton NMR spectra of

reaction products **IVa** and **IVb** do not contain a pyrrolium proton signal (9.76–10.10 ppm for the initial compound). All protons of the cyclooctadiene ring become non-equivalent and occur over a broad spectral range (1.5–4.92 ppm for **IVb**). In the ^{13}C NMR spectra, the carbon atoms directly bound to rhodium are responsible for doublets with spin–spin coupling constants of 5 and 13 Hz. The signal of the carbene

carbon atom appears as a doublet at 252 ppm with $^1J_{\text{CRh}} \approx 41$ Hz, which corresponds to published data for similar rhodium compounds [35]. The *ortho*-substituents in the aryl moiety remain non-equivalent. In the case of **IVb**, the CH₂ protons of the ethyl group also become non-equivalent and give rise to four ¹H NMR signals (1.50–1.93 ppm).

The donor ability of carbene ligands can be estimated by comparing the chemical shifts of the carbene carbon atom with those for known compounds (Scheme 4).



Scheme 4.

It can be seen from such an analysis that the signal for the carbene carbon atom in the ¹³C NMR spectra of the obtained complexes is a doublet with $\delta_{\text{C}} = 250$ ppm ($^1J_{\text{CRh}} \approx 41$ Hz), which is markedly greater than the corresponding values for rhodium complexes with the NHC group ($\delta_{\text{C}} \approx 190$ ppm) and lower than those for CAACs ($\delta_{\text{C}} \approx 278$ ppm) [23, 24, 35].

The structure of the obtained rhodium complexes was additionally confirmed in relation to compound **IVa** (Fig. 2) crystallized with one molecule of hexane, which was used to prepare the single crystals of suitable quality by slow evaporation from a hexane–dichloromethane mixture. According to X-ray diffraction data, the ferrocenyl moiety of **IVa** has a characteristic structure (Table 3), with Fe–C distances being in the range of 2.027(7)–2.071(7) Å and the angle between the corresponding aromatic planes being 3.316(5)°. The annulated pyrrole ring is virtually planar, as indicated by the mean deviation of atoms from the root-mean square plane, which is only 0.07(1) Å. 2,6-Dimethyl-substituted phenyl group is rotated relative to this plane by 85.1(3)°, which is attributable to the steric effect of bulky methyl substituents. The coordination geometry of rhodium formed by the pyrrole carbon atom, chloride anion, and the cyclooctadiene ligand resembles a trigonal prism (Table 3). This can be quantitatively described using the so-called “shape measures” [36], which characterize deviation of a coordination polyhedron from an ideal trigonal prism S(TP-6). The smaller this value, the better the polyhedron shape is described by the corresponding polyhedron. In complex **IVa**, the trigonal prismatic S(TP-6) “shape measure” estimated from X-ray dif-

fraction data using the Shape 2.1 program [36] is 10.080. For comparison, the corresponding deviations of the polyhedron shape from other ideal polyhedra (for example, a pentagonal pyramid or octahedron) with six vertices represented by four carbon atoms of the cyclooctadiene ligand, the pyrrole carbon atom, and the chloride anion are in the range of 17.822–25.243. The angle formed by the pyrrole nitrogen atom, carbene carbon atom, and the carbon atom of the cyclopentadienyl ring bound to carbene carbon (Fig. 2) in complex **IVa** (105.1(6)°) is smaller than in the case of CAACs (106.5°) [23, 34], so is the corresponding C(1)–C(2) bond length (1.457(10) Å versus 1.516 Å for CAACs). This bond is also shorter compared to those in analogous rhodium complexes (1.473 Å) containing an aromatic ring instead of ferrocene [35]). It is also noteworthy that, despite the presence of a large number of aromatic groups potentially capable of stacking interactions, no such interactions are present in the crystal of **IVa**.

Thus, it was shown that lithiation of ferrocenecarbaldehyde arylimines **Ia–Ic** involves the *ortho*-position to the imino group and gives a lithium salt able to react with benzophenone to give 1,2-disubstituted ferrocenes **IIa–IIc**. These products cyclize to give cationic complexes, precursors of ferrocene-containing carbenes **IIIa–IIIc**. On treatment with a base in the presence of [Rh(Cod)Cl]₂, these compounds form rhodium complexes with a new ferrocene-containing N-heterocyclic carbene. Analysis of structural data and shifts of ¹³C NMR signals of carbene carbon atoms shows that the electron-donor properties of carbene ligands in the complexes occupy an intermediate position between those of traditional imidazolium N-heterocyclic carbenes and cyclic alkyl(amino) carbenes CAACs.

ACKNOWLEDGMENTS

X-ray diffraction studies were supported by the Ministry of Science and Higher Education of the Russian Federation and were performed using research equipment of the Center for Studies of Molecular Structure of the Nesmeyanov Institute of Organoelement Compounds, Russian Academy of Sciences.

FUNDING

This study was supported by the Russian Science Foundation (project no. 18-73-00208).

CONFLICT OF INTEREST

The authors declare that they have no conflicts of interest.

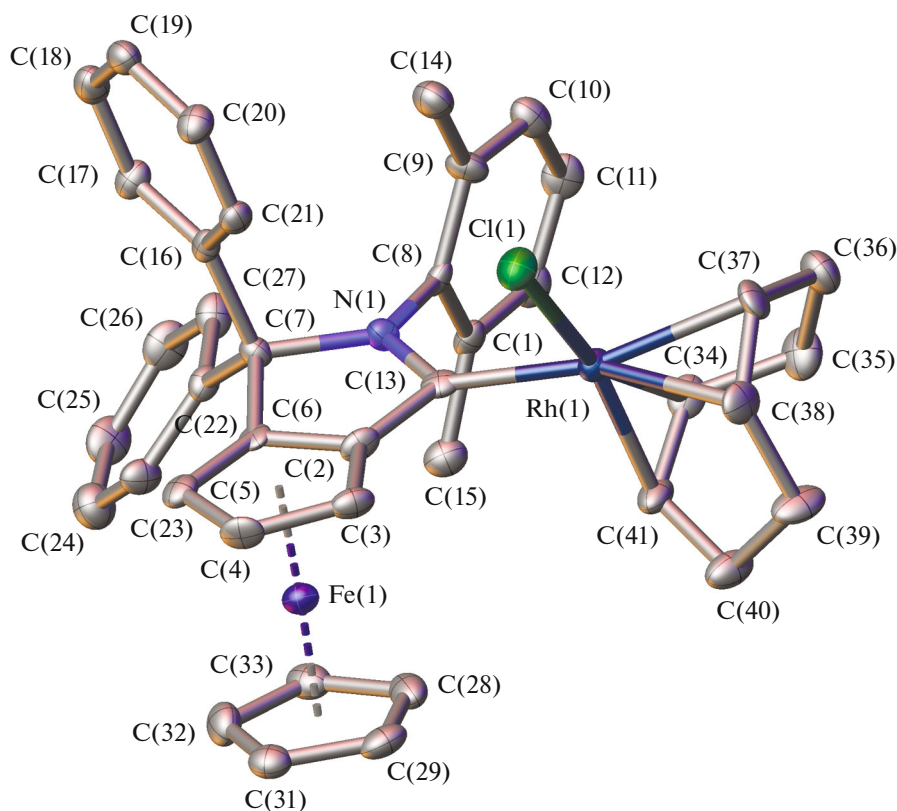


Fig. 2. General view of complex **IVa** with atoms being represented by thermal ellipsoids ($p = 50\%$). The solvate hexane molecule and hydrogen atoms are omitted for clarity.

Table 3. Selected geometric parameters of complex **IVa** according to X-ray diffraction data at 120 K*

Parameter	Value
Fe–C(Cp), Å	2.027(7)–2.071(7)
Rh–C(1), Å	2.012(7)
Rh–Cl(1), Å	2.372(2)
Rh–Cl(34), Å	2.129(7)
Rh–C(37), Å	2.205(7)
Rh–C(38), Å	2.208(7)
Rh–C(41), Å	2.106(7)
C(1)–C(2), Å	1.457(10)
N(1)C(1)C(2), deg	105.1(6)
α , deg	3.316(5)
β , deg	85.1(3)
S(TP-6)	10.080
S(PPY-6)	17.822
S(OC-6)	25.243

* C(Cp) stand for carbon atoms of the cyclopentadienyl rings; α is the angle between their root-mean square planes, β is the rotation angle of the 2,6-dimethyl-substituted phenyl group relative to the pyrrole plane. S(TP-6), S(PPY-6), S(OC-6) are deviations of the rhodium polyhedron shape from an ideal trigonal prism (TP-6), an ideal pentagonal pyramid (PPY-6), and an ideal octahedron (OC-6), respectively.

REFERENCES

1. Canary, J.W., *Chem. Soc. Rev.*, 2009, vol. 38, no. 3, p. 747.
2. *Molecular and Supramolecular Information Processing: From Molecular Switches to Unconventional Computing*, Katz, E., Ed., Weinheim Chichester: Wiley, 2012.
3. Sivaev, I., *Molecules*, 2017, vol. 22, no. 12, p. 2201.
4. *Molecular Switches*, Feringa, B.L. and Browne, W.R., Eds., Weinheim: Wiley-VCH, 2011.
5. Wang, X., Song, S., and Zhang, H., *Chem. Soc. Rev.*, 2020, vol. 49, no. 3, p. 736.
6. Blanco, V., Leigh, D.A., and Marcos, V., *Chem. Soc. Rev.*, 2015, vol. 44, no. 15, p. 5341.
7. Sims, C.M., Hanna, S.K., Heller, D.A., et al., *Nanoscale*, 2017, vol. 9, no. 40, p. 15226.
8. Al-Kutubi, H., Zafarani, H.R., Rassaei, L., and Mathwig, K., *Eur. Polym. J.*, 2016, vol. 83, p. 478.
9. Wu, T.-H., Hsu, Y.-Y., and Lin, S.-Y., *Small*, 2012, vol. 8, no. 13, p. 2099.
10. Sarkar, S., Dutta, S., Chakrabarti, S., et al., *ACS Appl. Mater. Interfaces*, 2014, vol. 6, no. 9, p. 6308.
11. Nikovskiy, I., Polezhaev, A., Novikov, V., et al., *Chem.-Eur. J.*, 2020, vol. 26, no. 25, p. 5629.
12. Pavlov, A.A., Aleshin, D.Y., Nikovskiy, I.A., et al., *Eur. J. Inorg. Chem.*, 2019, vol. 2019, no. 23, p. 2819.
13. Gallei, M. and Rüttiger, C., *Chem.-Eur. J.*, 2018, vol. 24, no. 40, p. 10006.

14. Wei, J. and Diaconescu, P.L., *Acc. Chem. Res.*, 2019, vol. 52, no. 2, p. 415.
15. Hopkinson, M.N., Richter, C., Schedler, M., and Glorius, F., *Nature*, 2014, vol. 510, no. 7506, p. 485.
16. Bourissou, D., Guerret, O., Gabbai, F.P., and Bertrand, G., *Chem. Rev.*, 2000, vol. 100, no. 1, p. 39.
17. Jacobsen, H., Correa, A., Poater, A., et al., *Coord. Chem. Rev.*, 2009, vol. 253, no. 5, p. 687.
18. Crudden, C.M. and Allen, D.P., *Coord. Chem. Rev.*, 2004, vol. 248, no. 21, p. 2247.
19. Crabtree, R.H., *Coord. Chem. Rev.*, 2013, vol. 257, no. 3, p. 755.
20. Huynh, H.V., *Chem. Rev.*, 2018, vol. 118, no. 19, p. 9457.
21. Díez-González, S. and Nolan, S.P., *Coord. Chem. Rev.*, 2007, vol. 251, no. 5, p. 874.
22. Gusev, D.G., *Organometallics*, 2009, vol. 28, no. 22, p. 6458.
23. Melaimi, M., Soleilhavoup, M., and Bertrand, G., *Angew. Chem., Int. Ed. Engl.*, 2010, vol. 49, no. 47, p. 8810.
24. Lavallo, V., Canac, Y., Präsang, C., et al., *Angew. Chem., Int. Ed. Engl.*, 2005, vol. 44, no. 35, p. 5705.
25. Nikovskiy, I.A., Spiridonov, K.A., Zakharova, D.V., et al., *Inorg. Chim. Acta*, 2019, vol. 495, p. 118976.
26. Polezhaev, A.V., Ezernitskaya, M.G., and Koridze, A.A., *Inorg. Chim. Acta*, 2019, vol. 496, p. 118844.
27. Koridze, A.A., Polezhaev, A.V., Safronov, S.V., et al., *Organometallics*, 2010, vol. 29, no. 19, p. 4360.
28. Polezhaev, A.V., Liss, C.J., Telser, J., et al., *Chem.-Eur. J.*, 2018, vol. 24, no. 6, p. 1330.
29. Sheldrick, G., *Acta Crystallogr., Sect. A: Found. Adv.*, 2015, vol. 71, no. 1, p. 3.
30. Dolomanov, O.V., Bourhis, L.J., Gildea, R.J., et al., *J. Appl. Crystallogr.*, 2009, vol. 42, no. 2, p. 339.
31. Peris, E., *Chem. Rev.*, 2018, vol. 118, no. 19, p. 9988.
32. Siemeling, U., *Eur. J. Inorg. Chem.*, 2012, vol. 2012, no. 22, p. 3523.
33. Takagaki, W., Yasue, R., and Yoshida, K., *Bull. Chem. Soc. Jpn.*, 2020, vol. 93, no. 2, p. 200.
34. Yoshida, K. and Yasue, R., *Chemistry*, 2018, vol. 24, no. 70, p. 18575.
35. Rao, B., Tang, H., Zeng, X., et al., *Angew. Chem., Int. Ed. Engl.*, 2015, vol. 54, no. 49, p. 14915.
36. Alvarez, S., *Chem. Rev.*, 2015, vol. 115, no. 24, p. 13447.

Translated by Z. Svitanko